Journal of Surface Analysis Vol.20, No. 3 (2014) pp. 207−210
M. Kubota et al. Depth Analysis of Ta/NiFe/Ta/CoFeB/Ta/NiFe Multilayer Thin Films: Comparison of Atom Probe Tomography and Auger Electron Spectroscopy

Paper

Depth Analysis of Ta/NiFe/Ta/CoFeB/Ta/NiFe Multilayer Thin Films: Comparison of Atom Probe Tomography and Auger Electron Spectroscopy

Masaki Kubota,[1]* Yoichi Ishida,[1] Katsuaki Yanagiuchi,[1] Hisashi Takamizawa,[2]
Yasuko Nozawa,[2] Naoki Ebisawa,[2] Yasuo Shimizu,[2] Takeshi Toyama,[2]
Koji Inoue,[2] and Yasuyoshi Nagai[2]
[1]*TDK Corporation, 543 Otai, Saku-shi, Nagano 385-8555, Japan*
[2]*The Oarai Center, Institute for Materials Research, Tohoku University, Oarai, Ibaraki 311-1313, Japan*
*mkubota@jp.tdk.com

(Received : December 24, 2013; Accepted : January 26, 2014)

Laser-assisted atom probe tomography (APT) and Auger electron spectroscopy (AES) were applied to examine the elemental distributions in Ta/NiFe/Ta/CoFeB/Ta/NiFe multilayer thin films. The impact of APT analysis direction on the elemental distributions of atoms which evaporate at high field could be seen. In particular, B atoms appeared deeper within the CoFeB layer along the analysis direction in APT due to its artifact. On the other hand, B atoms were homogeneously distributed in CoFeB layer with AES analysis.

1. Introduction

An investigation firm reported that digital data in the world will reach 40 Zetta Bytes (ZB: ten to the 21st power bytes) by 2020 [1]. It means the digital data in the world will increase to double in storage capacity every 2 years whether it stored in mobile PC or data center. In order to meet this demand, storage devices such as hard disk drives (HDDs) are required to be improved in their performances to reduce energy consumption.

Magnetic tunneling junctions (MTJs), such as CoFeB/MgO/CoFeB, are currently used in HDDs as an electronic component of reading sensor [2] and are of great interests because of their potential to the applications for the next generation current induced magnetization switching [3].

The functional properties of MTJs strongly depend on the chemical compositions across the interfaces, defect distribution, crystal structure of individual layer, interfacial roughness and layer thickness [4]. In particular, it has been reported that the B segregation from CoFeB amorphous layer toward the adjoining layers and subsequent crystallization into CoFe after a proper heat treatment is strongly related to the performance of MTJs [5-8]. Therefore, it is essential to characterize the elemental distribution with atomic scale resolution, and it is a key to reveal B distributions and the crystallization process of CoFeB.

Up to now, several studies have been made on characterizing B distributions in those multilayer systems by using a transmission electron microscopy (TEM) equipped with an electron energy loss spectroscopy (EELS) [9], an Auger electron spectroscopy (AES) [10] and X-ray photoelectron spectroscopy (XPS) [11]. However it is rather difficult to detect B by using those techniques in the analysis of multilayer thin films.

Laser-assisted atom probe tomography (APT) analysis allows the examination of local variation in elemental distribution on a sub-nanometer scale spatial resolution [12-15]. In addition, APT has a capability to detect light element, for example B. Therefore APT has been applied to the analysis of MTJs [16-18]. Moreover, there has been increasing demands for practical use of APT in the analyses of devices and materials in the wide variety of fields. Considering the practical use of APT for the MTJs, it is required to obtain accurate position of atoms. However it could be speculated that the position of atoms

obtained by APT is influenced by the analysis direction because of 1) the evaporation aberration around a crystal zone axis, 2) dissimilar evaporation fields between adjoining materials and 3) reconstruction algorism, etc [19-22].

In this study, APT was utilized to the analysis of B distribution in the model structure of CoFeB/Ta junctions with changing analysis direction anti-parallel and parallel to the film stacking direction as a standard and reversed analysis, respectively [18,23]. The obtained datasets were compared with that of AES with a low incident angle Ar beam by using inclined holder [24].

2. Experimental Procedure

In this study, the test stacking films consisting of Si-sub./Ta(1)/NiFe(5)/Ta(1)/CoFeB(5)/Ta(1)/

NiFe (nominal thicknesses in nanometers) were designed. All films were deposited by using DC magnetron sputtering system under Ar gas pressure on a cooling stage. In a similar method for site-specific specimen preparation based on focused ion beam (FIB) [25,26], wedge-style pieces including the region of interests were fabricated and extracted from the bulk. They were then mounted on preformed microtip arrays. For reversed analysis, lifted out wedge was rotated 180 degree by using rotation probe before mounting on the microtip arrays. After that they were sharpened under FIB annular milling (SIINT XVision 200TB) of 5 kV Ga^+ so that the final tip radius was less than 50 nm. These needle shaped specimens were analyzed by using CAMECA LEAP 4000XHR applying 10 pJ of UV laser (wavelength: 355 nm) at a rate of 200 kHz and data detection rate of 0.002 per pulse. During the measurements specimens were cooled at around 35 K to prevent from surface migration of the atoms. For AES, CoFeB layer was additionally sputter-deposited on the test staking films in order to distinguish between B and Ta spectra by performing data treatment with linear least square fitting [27,28]. Then sputter depth profiling for the specimen was performed by using ULVAC-PHI SAM-680 with a low incident angle Ar ion beam. To achieve this analysis, an 85 degree inclined holder was specially made. The incident electron beam current was 8 nA at 10 kV. 1 mm × 1mm in area was irradiated by 1 kV of Ar ion beam with the incident angle of 87 degree during the analysis. Prior to these analyses, TEM observation was carried out by using JEOL JEM-ARM200F.

3. Results and Discussion

In Fig. 1, cross-sectional TEM image of the test stacking films was shown. As you can see, CoFeB layer had amorphous structure, suggesting homogeneous distribution of B in the CoFeB layer [8].

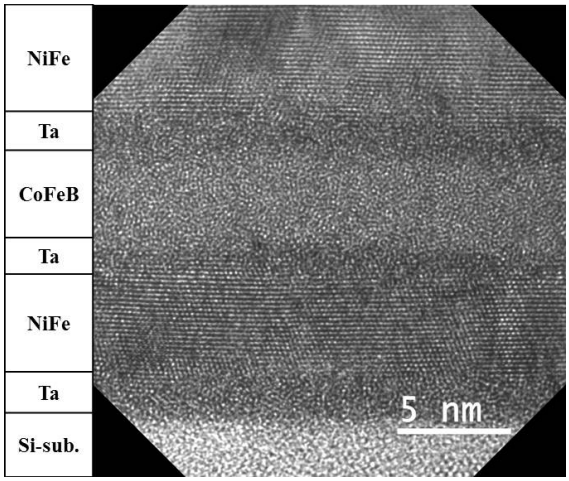

Fig. 1 Schematic cross-section diagram and TEM image of the test stacking films.

Figure 2 shows 1D composition depth profiles obtained by APT with the analysis anti-parallel (standard) and parallel (reversed) to the film stacking direction. In the standard analysis (Fig. 2a), it could be seen that B concentration reached its peak at the interface between CoFeB and Ta adjacent to the underside of the CoFeB layer while Fe distribution in the CoFeB layer was relatively homogeneous. On the other hand, B concentration shown in Fig. 2b reached its peak at the interface of CoFeB layer and Ta layer adjacent to upper side of the CoFeB layer with reversed analysis. These results suggest that B atoms appeared deeper along the analysis direction. The Ta profile also exhibited increasing slopes along the analysis direction.

The evaporation field of B^+, Ta^{+++}, Co^{++}, Ni^{++}, Fe^{++} and Si^{++}, which are mainly detected charge states, are 64, 44, 37, 36, 33 and 33 V/nm, respectively [29]. B and Ta could be classified in high field element. Therefore, the atoms which evaporate at higher field tend to be detected later than that evaporate at lower field. The detailed mechanism of this phenomenon has not been clarified yet. However we can speculate that field-assisted surface migration and changes in the specimen tip shape through

the interfaces affected the position of atoms [30].

Figure 3 shows 1D composition depth profiles obtained by AES. In this figure, the Co profile was shown by subtracting overlapped Ni spectra from the original Co spectra. It could be seen that the B atoms were widely distributed in CoFeB layer. Focusing on Ta profile, the decay length was longer than that in APT analysis. In this measurement, high voltage of the incident ion was 1 kV. It must be too low to remove Ta from the specimen surface. In order to achieve sputter depth profiling in high resolution by AES, higher voltage for incident ion must be required in this test stacking films. Although the spatial resolution of AES is lower than that of APT, we found that the order of the atoms obtained by AES is more accurate.

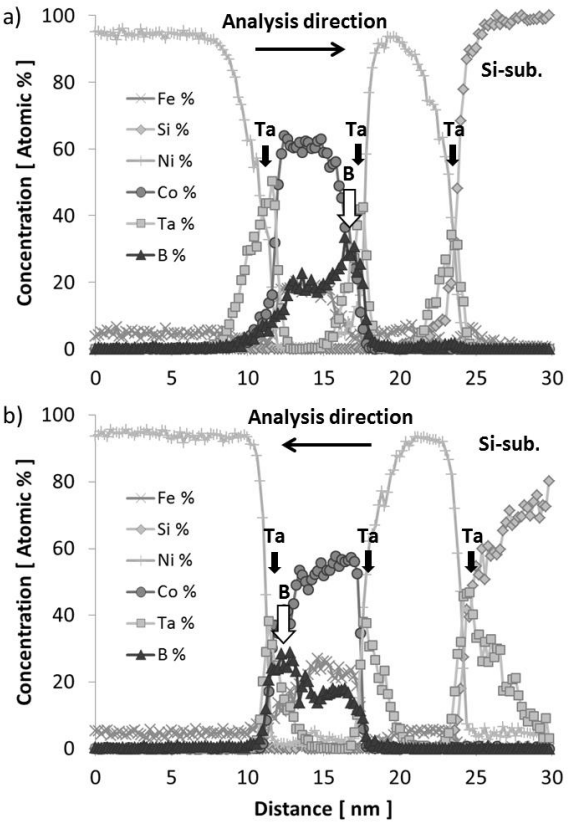

Fig. 2 1D composition depth profiles of the test stacking films by APT with the analysis direction a) anti-parallel (standard) and b) parallel (reversed) to the film stacking direction.

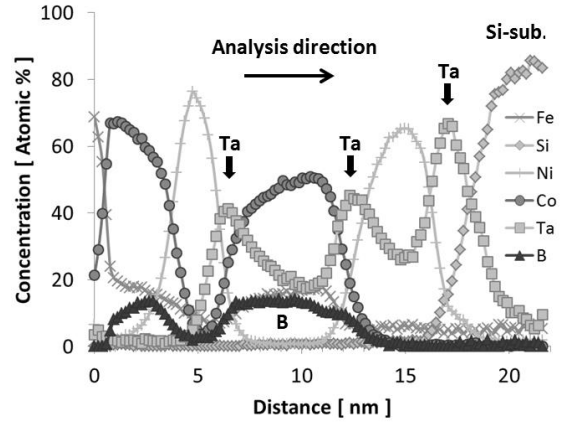

Fig. 3 1D composition depth profiles of the test stacking films obtained by AES with a low incident angle Ar ion beam.

4. Conclusions

Ta/NiFe/Ta/CoFeB/Ta/NiFe structures have been analyzed by using APT and AES. In APT analysis with the analysis direction anti-parallel to the film stacking direction, B appeared deeper along the analysis direction within the CoFeB layer. The same tendency was observed in the analysis parallel to the film stacking direction. On the other hand, AES has shown homogeneous B distribution within the CoFeB layer. These results indicate that APT should be employed in conjunction with other analysis techniques as a complementary approach to the analysis of microstructural feature and local elemental distributions in multilayer systems.

5. Acknowledgements

The authors acknowledge S. Kawasaki, H. Takahashi, Y. Miura, K. Makino, S. Miura, K. Edagawa, and K. Hirata for sample preparation and for helpful discussions.

6. References

[1] J. Gantz and D. Reinsel, IDC view “Big Data, Bigger Digital Shadows, and Biggest Growth in the Far East” (2012).

[2] T. Kagami, T. Kuwashima, S. Miura, T. Uesugi, K. Barada, N. Ohta, N. Kasahara, K. Sato, T. Kanaya, H. Kiyono, N. Hachisuka, S. Saruki, K. Inage, N. Takahashi, and K. Terunuma, *IEEE Trans. Magn*., **42**, 93 (2006).

[3] S. Ikeda, K. Miura, H. Yamamoto, K. Mizunuma, H. D. Gan, M. Endo, S. Knai, J. Hayakawa, F. Matsukura, and H. Ohno, *Nature Mater.* **9**, 721 (2010).

[4] Y. M. Lee, J. Hayakawa, S. Ikeda, F. Matsukura, and H. Ohno, *Appl. Phys. Lett.* **90**, 212507 (2007).

[5] D. D. Djayaprawira, K. Tsunekawa, M. Nagai, H. Maehara, S. Yamagata, N. Watanabe, S. Yuasa, Y. Suzuki, and K. Ando, *Appl. Phys. Lett.* **86**, 092502 (2005).

[6] D. J. Kim, J. Y. Bae, W. C. Lim, K. W. Kim, and T. D. Lee, *J. Appl. Phys.* **101**, 09B505 (2007).

[7] T. Ibusuki, T. Miyajima, S. Umehara, S. Eguchi, and M. Sato, *Appl. Phys. Lett.* **94**, 062509 (2009)

[8] T. Miyajima, T. Ibusuki, S. Umehara, M. Sato, S. Eguchi, M. Tsukada, and Y. Kataoka, *Appl. Phys. Lett.* **94**, 122501 (2009).

[9] J. J. Cha, J. C. Read, R. A. Buhrman, and D. A. Muller, *Appl. Phys. Lett.* **91**, 062516 (2007).

[10] D. K. Kim, J. U. Cho, B. S. Chun, K. H. Shin, K. J. Lee, M. Tsunoda, M. Takahashi, and Y. K. Kim, *Appl. Phys. Lett.* **101**, 232401 (2012).

[11] J. Y. Bae, W. C. Lim, H. J. Kim, T. D. Lee, K. W. Kim, and T. W. Kim, *J. Appl. Phys.* **99**, 08T316 (2006).

[12] B. Gault, F. Vurpillot, A. Vella, M. Gilbert, A. Menand, D. Blavette, and B. Deconihout, *Rev. Sci. Instrum.* **77**, 043705 (2006).

[13] T. F. Kelly and M. K. Miller, *Rev. Sci. Instrum.* **78**, 031101 (2007).

[14] K. Hono, T. Ohkubo, Y. M. Chen, M. Kodzuka, K. Oh-ishi, H. Sepehri-Amin, F. Li, T. Kinno, S. Tomiya, and Y. Kanitani, *Ultramicroscopy* **111**, 576 (2011).

[15] D. J. Larson, D. Lawrence, W. Lefebvre, D. Olson, T. J. Prosa, D. A. Reinhard, R. M. Ulfig, P. H. Clifton, J. H. Bunton, D. Lenz, J. D. Olson, L. Renaud, I. Martin, and T. F. Kelly, *J. Phys. Conf. Ser.* **326**, 012030 (2011).

[16] S. Pinitsoontorn, A. Cerezo, A. K. Petford-Ling, D. Mauri, L. Folks, and M. J. Carey, *Appl. Phys. Lett.* **93**, 071901 (2008).

[17] H. Bouchikhaoui, P. Stender, D. Akemeier, D. Baither, K. Hono, and A. Hütten, *Appl. Phys. Lett.* **103**, 142412 (2013).

[18] M. Kubota, Y. Ishida, K. Yanagiuchi, H. Takamizawa, Y. Nozawa, Y. Shimizu, T. Toyama, K. Inoue, and Y. Nagai, Abstract of 2013 *JSAP-MRS Joint Symposia*, Kyoto, Japan (2013).

[19] M. K. Miller, *Atom Probe Tomography: Analysis at the Atomic Level*, Springer, New York (2000).

[20] F. Vurpillot, A. Bostel, and D. Blavette, *Appl. Phys. Lett.* **76**, 3127 (2000).

[21] M. K. Miller, M. G. Hetherington, *Surf. Sci.* **246**, 442 (1991).

[22] F. Vurpillot, A. Cerezo, D. Blavette, and D. J. Larson, *Microsc. Microanal.* **10**, 384 (2004).

[23] D. J. Larson, T. J. Prosa, B. P. Geiser, and W. F. Egelhoff Jr., *Ultramicroscopy* **111**, 506 (2011).

[24] T. Ogiwara, T. Nagatomi, K. J. KIM, and S. Tanuma, *J. Surf. Anal.* **18**, 174 (2012).

[25] D. J. Larson, D. T. Foord, A. K. Petford-Long, A. Cerezo, G. D. W. Smith, *Nanotechnology* **10**, 45 (1999).

[26] D. J. Larson, D. T. Foord, A. K. Petford-Long, H. Liew, M. G. Blamire, A.Cerezo, G. D. W. Smith, *Ultramicroscopy* **79**, 287 (1999).

[27] D. G. Watson, *Surf. Interface Anal.* **14**, 59 (1989).

[28] K. Yanagiuchi, Proceedings of Nagano mogel 99': *The Second MAGNETO-ELECTRONICS International Symposium*, 263 (1999).

[29] T. T. Tsong, *Surf. Sci.* **70**, 211 (1978).

[30] D. J. Larson, B. P. Geiser, T. J. Prosa, S. S. A. Gerstl, D. A. Reinhard, and T. F. Kelly, *J. Microsc.* **243**, 15 (2010).